

Supported Cobalt Oxide Nanoparticles As Catalyst for Aerobic Oxidation of Alcohols in Liquid Phase

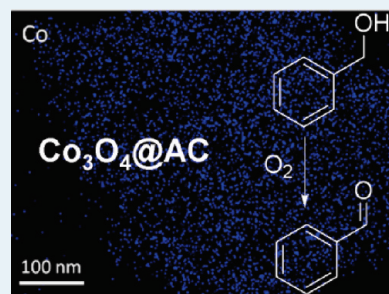
Junjiang Zhu,* Kamalakannan Kailasam, Anna Fischer, and Arne Thomas*

Technische Universität Berlin, Englische Strasse 20, 10587 Berlin, Germany

S Supporting Information

ABSTRACT: Supported cobalt oxide nanoparticles (NPs) have been prepared by wetness impregnation on different supports and subsequent heat treatment in argon at 350 °C for 2 h. The thus prepared cobalt oxide (Co_3O_4) can be well dispersed on carbonaceous materials such as activated carbon (AC) and covalent triazine frameworks (CTF), with average particle sizes below 5 nm. The catalytic performance of supported Co_3O_4 NPs was tested by aerobic oxidation of alcohols in liquid phase. The results show that AC supported Co_3O_4 NPs, $\text{Co}_3\text{O}_4/\text{AC}$, exhibit $\sim 100\%$ conversions for alcohol oxidation and can be reused for at least 4 runs without appreciable loss of activity, when a thermal regeneration step is carried out, suggesting that the Co_3O_4 NPs are well embedded and stabilized on the support, making $\text{Co}_3\text{O}_4/\text{AC}$ a promising catalyst for aerobic oxidation of alcohols in liquid phase.

KEYWORDS: activated carbon, cobalt oxide, nanoparticles, alcohol oxidation, liquid phase



INTRODUCTION

The effect of the particle size on the catalytic performance of materials is of main scientific and industrial importance.¹ The preparation of particles with nanometer dimensions for catalytic applications has received intensive attention in recent decades, as nanoparticles (NPs) not only show high surface to volume ratios but also different chemical and physical properties compared with the bulk. For example, it was frequently shown that the catalytic performance of metal particles, either supported or unsupported, depend closely on their size and/or shape in various catalytic reactions.^{2–6} This is especially true for gold catalyst, where just gold nanoparticles showed activity for certain catalytic reactions.^{7–9} Beside noble metals, also the catalytic performances of base metal (oxides) have been shown to be largely dependent on the particle size.^{10–15} For example, Lee et al.¹¹ recently reported that the activity of Fischer–Tropsch reaction depends closely on the particle size of iron oxide, and at the particle size of ~ 6.2 nm the catalyst shows the best activity.

In the case of supported particles, the control of particle size undoubtedly is closely related to the type of support used. The application of supports with smaller pores and higher surface areas and additionally a favorable interaction with the particles is preferable to prepare smaller NPs directly on the support. Particles can be well dispersed on higher surface areas and the leaching of particles decreases if there is a strong affinity between the support and the particles. In catalysis, beside the size of the metal particles the properties of the support also need to be considered, as the support can influence the electronic structure of the supported NPs and/or interfere in the catalytic reaction by itself.^{16–19} As example, for carbon materials, commonly used as catalyst support, the surface functional groups of the carbon can

act as active site of oxygen activation in catalytic oxidation reaction.^{20–23}

In this work, formation of cobalt oxide on carbonaceous materials such as activated carbon (AC) and covalent triazine frameworks (CTF) was investigated. Cobalt oxide is a good catalyst for various reactions,^{19,24–33} such as dehydrogenation,^{25,26,28} VOC combustion,^{19,33} alcohol oxidation,²⁹ CO oxidation,^{30,32} and others. AC is a well-known support for various catalytic NPs, and CTF also was recently proven to be an attractive catalyst support for various reactions.^{34–37} Here the catalytic performance of supported Co_3O_4 catalysts was tested for the selective aerobic oxidation of alcohols in liquid phase, which is an important reaction in organic chemistry for the synthesis of chemical intermediates, using green and clean chemicals. Comparing with the normal gold catalysts, carried out in basic conditions,³⁸ the here reported $\text{Co}_3\text{O}_4/\text{AC}$ catalyst show $\sim 100\%$ alcohol conversion even in the absence of any promoter (e.g., NaOH), and further can be reused for at least 4 runs without appreciable loss in activity when an additional thermal regeneration step is carried out, indicating that $\text{Co}_3\text{O}_4/\text{AC}$ is a very promising candidate for aerobic oxidation of alcohols in liquid phase.

RESULTS AND DISCUSSION

Figure 1 shows the X-ray diffraction (XRD) patterns of cobalt oxide supported on AC and CTF (i.e., $\text{Co}_3\text{O}_4/\text{AC}$ and $\text{Co}_3\text{O}_4/\text{CTF}$). The intensities of the diffraction peaks of both samples are

Received: December 23, 2010

Revised: February 9, 2011

Published: March 02, 2011

very weak, which imply that the cobalt oxides formed on the supports are mainly amorphous or that very small particles are formed, making the attribution of the diffraction peaks to a distinct cobalt oxide phase, for example, CoO, Co₂O₃, or Co₃O₄, impossible. To verify the possible product formed during the thermal treatment, the XRD patterns of a bulk sample, prepared by the same procedure but without support, were also taken, showing that Co₃O₄ is the product under these conditions. Thus, it can be assumed that the cobalt oxides prepared on the support mainly consist of Co₃O₄.

XPS measurements were carried out to obtain further insight into the oxidation state of cobalt in the AC supported catalyst. Figure 2a shows the peak of Co2p_{3/2} located at ~780 eV and that of Co2p_{1/2} at ~796 eV. After deconvolution it can be seen that the peak of Co³⁺ locates at ~779.8 eV and that of Co²⁺ at ~781.5 eV, which are in good accordance with that observed from single Co₃O₄ (~779.5 eV for Co³⁺ and ~780.8 eV for Co²⁺).^{39–42} The peak location of O1s (Figure 2b) however is higher than that observed from the reported Co₃O₄,^{39–42} but could be also attributed to the oxygen in the surface groups of the carbon support, which usually show high binding energy in the range of 531–534 eV.^{43,44} Still, after deconvolution the first peak is found to be located at ~530 eV, which is similar to that observed from Co₃O₄,^{39–42} while the other three peaks located at ~531, ~533, and 534 eV, according to Figueiredo et al.,⁴³ can be assigned to carbonyl (or quinine), anhydride (or lactone), and carboxylic groups on the carbon surface, respectively.

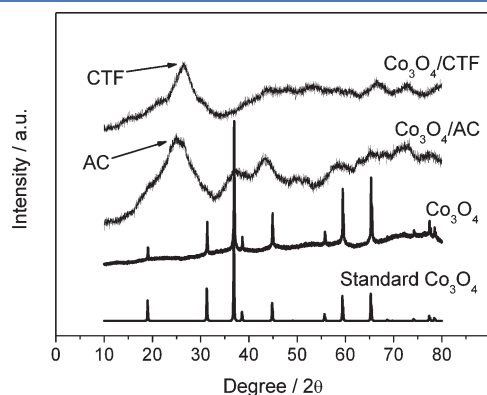


Figure 1. XRD patterns of the supported cobalt oxide catalysts and Co₃O₄ as reference.

Thermogravimetric analysis (TGA) measurements on the catalysts (Figure 3) show a significant decrease in the thermal stability of the supports after loading with Co₃O₄. This can be attributed to the catalytic activity of the cobalt oxide NPs for the oxidation of the supports. CTF is more stable against decomposition than the AC support, showing higher oxidation stability, which have been also reported for other nitrogen-rich carbon materials.^{45–47} Nevertheless, both catalysts are stable in O₂ atmosphere at temperatures below 200 °C, and thus can be used in liquid phase reactions without concerns about their thermal stabilities. From the remaining weight after TGA experiments, it can be calculated that the Co₃O₄ loading in the catalyst is ~13 wt %.

To further reveal the structure of the catalysts, TEM measurements were carried out on Co₃O₄/AC and Co₃O₄/CTF (Supporting Information, Figure S1). However in this BF-TEM mode, no metal oxide particles could be observed for both catalysts, although Co was undoubtedly detected in the EDX analysis (see Supporting Information, Figure S1c). This suggests that the supported Co₃O₄ particles are either very small and/or poorly crystalline or both, as the contrast are governed by mass thickness and diffraction. This is in line with the weak intensity of diffraction peaks and rings observed in XRD and electron diffraction measurements, respectively. Therefore high-angle annular dark field-scanning TEM (HAADF-STEM) was performed (Z-contrast), allowing the imaging of the Co₃O₄ particles with high atomic numbers in a matrix of light elements, such as

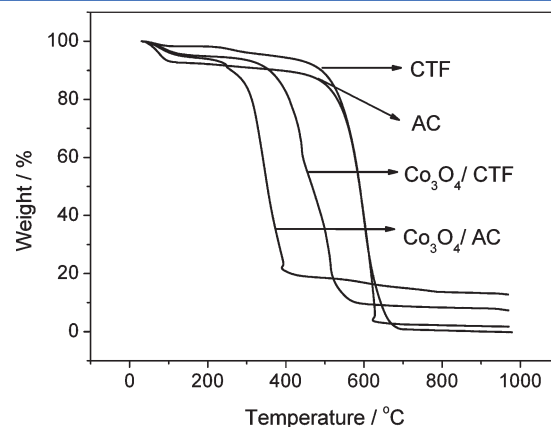


Figure 3. TGA curves of the supports (AC and CTF) and the corresponding cobalt oxide catalysts.

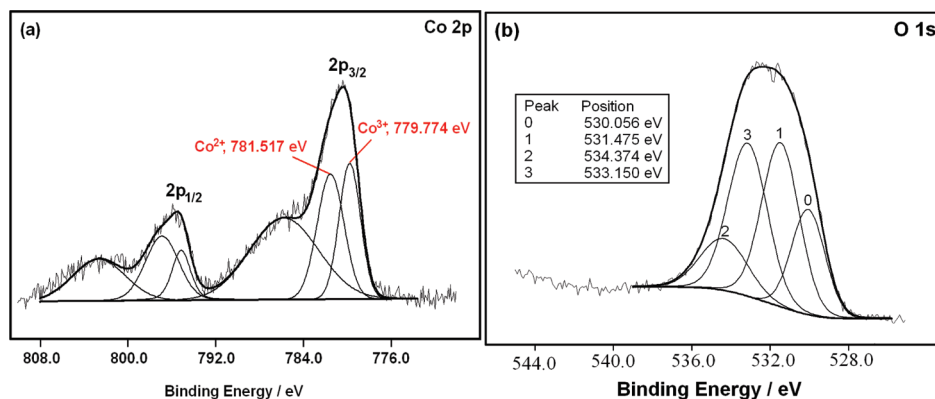


Figure 2. Co2p (a) and O1s (b) XPS spectra of the Co₃O₄/AC catalyst.

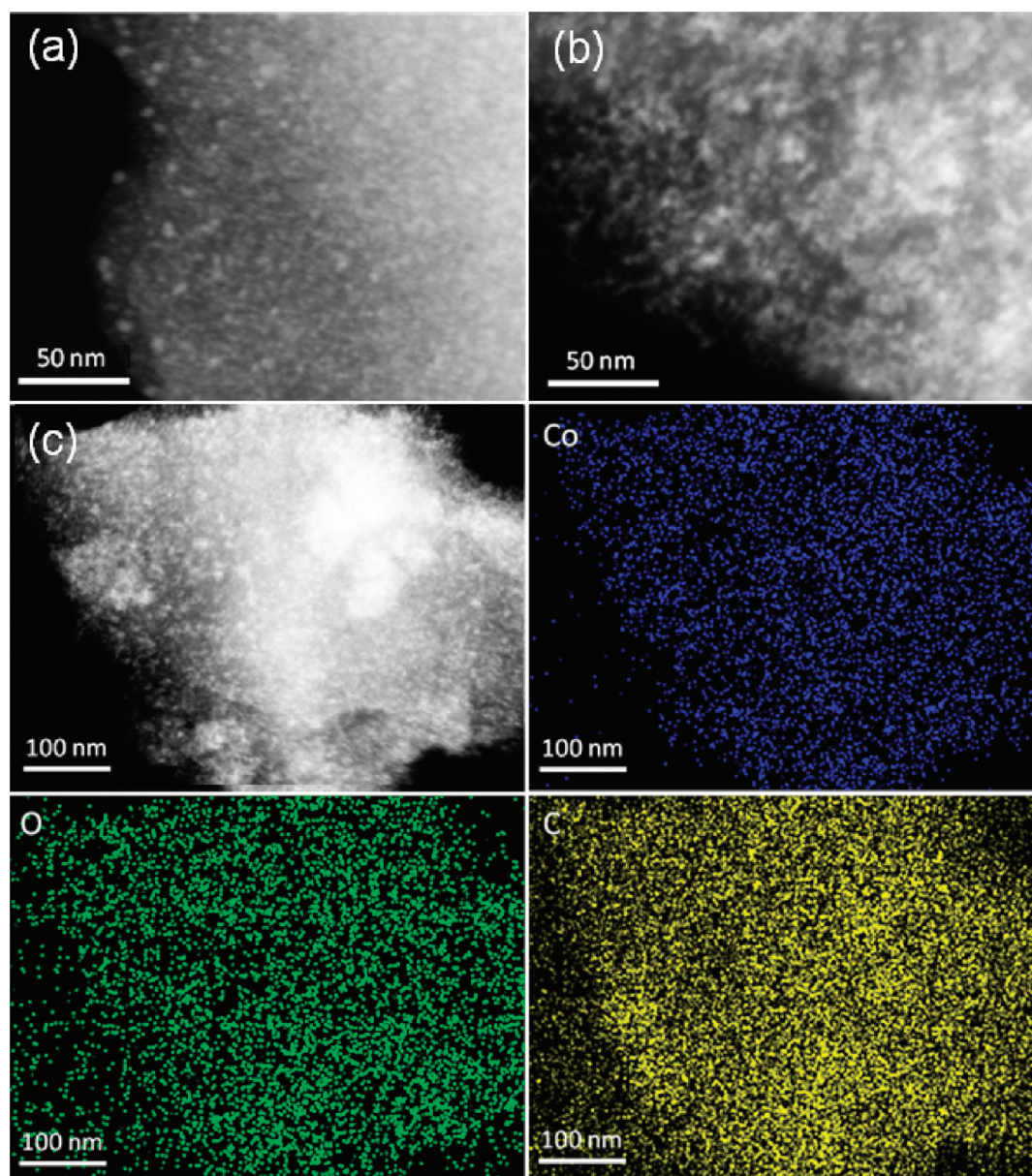


Figure 4. STEM images of samples (a) $\text{Co}_3\text{O}_4/\text{AC}$ and (b) $\text{Co}_3\text{O}_4/\text{CTF}$, and (c) the corresponding Co, C, and O-EDX mapping.

Table 1. Textural Properties and Catalytic Performances of the Investigated Samples

sample	textural properties		activity at $t = 3$ h	
	S.A. (m^2/g) ^a	P.V. (cm^3/g) ^b	alcohol conv. (%)	aldehyde sel. (%) ^c
AC	875	0.42	18.5	0 ^d
CTF	677	0.38	11.2	0 ^d
HSA_CTF	2849	1.98	15.7	0 ^d
Co_3O_4	18		32.2	50.3
$\text{Co}_3\text{O}_4/\text{AC}$	597	0.32	~ 100 ^e	87.3
$\text{Co}_3\text{O}_4/\text{CTF}$	392	0.24	17.8	25.2
$\text{Co}_3\text{O}_4/\text{HSA_CTF}$	987	0.52	61.0	51.8

^a BET surface area determined by BET method (5 points). ^b Pore volume determined at $P/P_0 = 0.99$. ^c Trace amount of reactant was out of the detection limitation of GC-MS. ^d The amount of product being formed is out of the detection limitation of GC-MS. ^e Possible byproduct such as toluene cannot be excluded in the reaction.

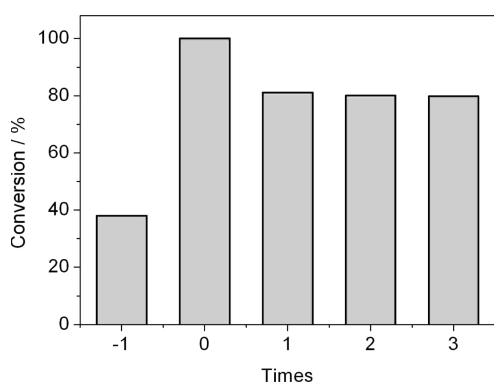


Figure 5. Long-term stability of $\text{Co}_3\text{O}_4/\text{AC}$ catalyst in selective oxidation of benzyl alcohol using molecular oxygen; “-1”: The reused catalyst is dried in air at 100°C ; “0”: Here fresh catalyst is used; “1, 2, and 3”: The reused catalyst is treated in Ar at 350°C for 2 h.

AC or CTF. As seen from Figure 4, on both supports small Co_3O_4 NPs with average particle sizes below 5 nm are homogeneously dispersed. This is further supported by EDX mapping of the $\text{Co}_3\text{O}_4/\text{CTF}$ catalyst (Figure 4c).

In Table 1 the porous characteristics of the studied catalysts are listed. N_2 -sorption measurements show that both AC and CTF are microporous materials, with a Brunauer–Emmett–Teller (BET) surface area of 875 and $677\text{ m}^2/\text{g}$, respectively. The surface area of both materials decreases after loading with cobalt oxide catalysts, but still has considerable values of 597 and $392\text{ m}^2/\text{g}$, indicating that most of the pores are still accessible.

The structure of the materials, that is, small Co_3O_4 particles supported homogeneously on a high surface area support suggest that they might be effective heterogeneous catalysts. Indeed, it was found that $\text{Co}_3\text{O}_4/\text{AC}$ can show $\sim 100\%$ conversion (see Table 1) for aerobic oxidation of benzyl alcohol, which is one of the most used test reactions in liquid phase.⁴⁸ Also, it was found that the activity of $\text{Co}_3\text{O}_4/\text{AC}$ is far higher than that of $\text{Co}_3\text{O}_4/\text{CTF}$, which is different from the trends observed on noble metal catalyst (e.g., Pd/AC vs Pd/CTF).³⁴ It should be, however, noted that in the latter study a high surface area CTF (denoted here as: HSA_CTF) was used, which is prepared at higher temperatures,⁴⁹ while in here we first used a periodic CTF,⁵⁰ to compare materials with similar surface areas. Using a HSA_CTF as support of Co_3O_4 show an increased activity compared to the low-surface area one (CTF), but still the activity is lower than that of $\text{Co}_3\text{O}_4/\text{AC}$ (see Table 1).

The difference in the activity of $\text{Co}_3\text{O}_4/\text{AC}$ and $\text{Co}_3\text{O}_4/\text{CTF}$ could be due to the higher oxidation stability of the nitrogen-rich CTFs compared to AC. Surface oxygen species found on the termination sites of AC can probably participate in the reaction and are subsequently regenerated by molecular oxygen,^{20–23} while for CTFs with higher oxidation stability only few or even none of such surface oxygen sites are available and hence low activity is observed. Furthermore, Co_3O_4 seems to form larger aggregates of particles on the CTF than on the AC support, as seen from the STEM images, which might yield a lower active metal surface area.

The different trends in the catalytic performances observed from metal oxides and noble metals supported on these two supports^{34,37} could be partially due to the different alcohols used in these two systems. Still the reversal in the trends could also point to a different reaction mechanism in these two catalytic systems. Besides, for the supported cobalt oxide catalysts, the

reaction proceeds in a neutral medium, in which both the alcohol and the oxygen are activated by the catalyst. The reaction mechanism of alcohol oxidation carried out on metal oxide catalysts supported on AC is the subject of our current work.

To check the stability of the Co_3O_4 NPs and verify that the reaction is predominantly heterogeneous, a leaching experiment was carried out:^{51,52} after 1 h of reaction, the catalyst ($\text{Co}_3\text{O}_4/\text{AC}$) was filtered and the reaction was left to continue for another 1 h, the conversions measured before and after filtering were 64.9% and 63.3%, thus practically the same within experimental error, showing that the reaction is mainly heterogeneous. Certainly, it can not be excluded that very low levels of cobalt oxide could leach during the reaction, as it was carried out in liquid phase, and that cobalt oxide may be active for the reaction with short lifetime. [We thank Prof. Graham Hutchings in Cardiff University for discussing with this possibility with us.] For this, a TGA test on $\text{Co}_3\text{O}_4/\text{AC}$ before and after reaction was carried out and shown in the Supporting Information, Figure S5, showing no significant weight loss of Co_3O_4 . This is in line with what was reported in previous works,^{53,54} where cobalt leaching is also not detectable. Hence, we considered that the Co_3O_4 NPs are well embedded on the AC support, and cobalt leaching could be neglected, that is, the reaction is predominantly heterogeneous.

The stability of $\text{Co}_3\text{O}_4/\text{AC}$ catalyst for alcohol oxidation was also investigated by recycling tests. The results in Figure 5 show that the activity is decreased if the reused catalyst is only dried in air at 100°C (denoted as “-1”). However, considerable activity ($\sim 80\%$) can still be obtained when the reused catalyst is treated again in Ar at 350°C for 2 h (like the treatment of the fresh catalyst), and no appreciable loss in the activity is observed after the second run. This indicates that the Co_3O_4 NPs on AC are very stable and $\text{Co}_3\text{O}_4/\text{AC}$ catalyst has good reusability for liquid phase alcohol oxidation reaction. Also, it was found that the $\text{Co}_3\text{O}_4/\text{AC}$ catalyst is not only active for the oxidation of benzyl alcohols but also for a range of other alcohols yielding the respective aldehydes and ketones, as listed in the Supporting Information, Table S1.

CONCLUSIONS

In summary, we have shown that supported cobalt oxide particles with diameters below 5 nm can be prepared through a wetness impregnation method on different supports. $\text{Co}_3\text{O}_4/\text{AC}$ is a suitable catalyst for liquid phase alcohol oxidation carried out in neutral medium and can be recycled well after a thermal treatment. Results shown here suggest that supported metal oxide catalyst such as $\text{Co}_3\text{O}_4/\text{AC}$ can replace noble metals when used for alcohol oxidation reaction, and hence offers a more economic way of producing organics in industrial plants.

EXPERIMENTAL SECTION

Preparation of Catalysts. AC (moisture: 17.98%, ash: 3.41%, BET surface area: $875\text{ m}^2/\text{g}$) was purchased from Degussa and metal nitrates from Sigma Aldrich. CTF and high surface area CTF (denoted as HSA_CTF) were prepared according to references.^{48,49} The supported cobalt oxide catalysts (Loading: $\sim 13\text{ wt } \%$) were prepared by wetness impregnation method: 0.5 g of $\text{Co}(\text{NO}_3)_2 \cdot 6\text{H}_2\text{O}$ was first dissolved in 5 mL of deionized water; to this solution 1 g of support (AC, CTF or HSA_CTF) was added. The resulting slurry was dried in a static-air oven at

110 °C overnight and then thermally treated in Ar at 350 °C for 2 h (heating rate of 5 °C min⁻¹) in a muffle oven.

Characterization of Catalysts. XRD patterns were collected in a Bruker D8 Advance X-ray diffractometer using Cu K α 1 irradiation (λ = 0.154 nm). BET surface areas were obtained from the N₂ sorption isotherms, determined at liquid nitrogen temperature (−196 °C) with an Autosorb-1 equipment. TGA curves were measured on a PerkinElmer STA 6000 instrument in oxygen atmosphere. The oxygen flow rate is 20 mL min⁻¹, and the heating rate of the sample is 10 °C min⁻¹. For the used catalysts, they were dried in a static-air oven at 110 °C overnight before performing the TGA experiment. TEM images were obtained from a FEI Tecnai 20 microscope, using carbon-coated copper grids. BF TEM was performed on a Zeiss EM Omega 912X at an acceleration voltage of 120 kV. HAADF-TEM measurements were performed on a LIBRA 200 (Zeiss) operated at 200 kV and equipped with an EDX detector from Thermo Fischer operated with the “System 6” software. XPS analysis was performed with a VG Scientific ESCALAB 200A spectrometer using non-monochromatized Mg K α radiation (1253.6 eV). The charging effect was corrected using the C 1s level (285.0 eV) as a reference.

Catalytic Tests. The reaction was carried out at atmospheric pressure, in a 50 mL, three-necked batch reactor fitted with a reflux condenser, oil bath, thermocouple, and magnetic stirrer. A typical reaction condition was 20 mL of toluene, 20 μ L of benzyl alcohol, 10 μ L of decane (internal standard); 0.1 g of catalysts; oxygen flow rate is 50 mL min⁻¹; purity of oxygen is 99.99%; reaction temperature is 80 °C and reaction time is 3 h. The products were analyzed by an Agilent 7890A/5975C GC-MS. The catalytic activity was calculated as follows:³⁷ % Conv = 100 \times ([C₀] − [C₁])/[C₀]; Selectivity to benzaldehyde = 100 \times [C′]/([C₀] − [C₁]), where [C₀] and [C₁] are the initial and final molar concentrations of the benzyl alcohol, and [C′] is the molar concentration of benzaldehyde formed during the reaction.

■ ASSOCIATED CONTENT

Supporting Information. Additional characteristic results, such as TEM images, EDX analysis, TGA curves; alcohol conversion with reaction time; reaction rate of different catalysts for alcohol oxidation; a higher magnification STEM image (scale bar of 20 nm) of the Co₃O₄/AC; direct activity profiles obtained from GC-MS; and the activities of Co₃O₄/AC for various alcohol oxidation. This material is available free of charge via the Internet at <http://pubs.acs.org>.

■ AUTHOR INFORMATION

Corresponding Author

*E-mail: ciaczj@gmail.com (J.Z.), arne.thomas@tu-berlin.de (A.T.).

Funding Sources

Financial support from the German Research Foundation (DFG, Grant TH 1463/5-1) and the Cluster of Excellence “Unifying Concepts in Catalysis” (EXL 31411) are gratefully acknowledged.

■ ACKNOWLEDGMENT

Dr. Markus Wollgarten from the Helmholtz-Zentrum Berlin is acknowledged for the access to the LIBRA 200 EM.

■ REFERENCES

- (1) den Breejen, J. P.; Radstake, P. B.; Bezemer, G. L.; Bitter, J. H.; Froese, V.; Holmen, A.; de Jong, K. P. *J. Am. Chem. Soc.* **2009**, *131*, 7197–7203.
- (2) Che, M.; Bennett, C. O. *Adv. Catal.* **1989**, *36*, 55–172.
- (3) Henry, C. R. *Surf. Sci. Rep.* **1998**, *31*, 235–325.
- (4) Somorjai, G. A.; Tao, F.; Park, J. Y. *Top. Catal.* **2008**, *47*, 1–14.
- (5) Van Santen, R. A. *Acc. Chem. Res.* **2009**, *42*, 57–66.
- (6) Bezemer, G. L.; Bitter, J. H.; Kuipers, H. P. C. E.; Oosterbeek, H.; Holewijn, J. E.; Xu, X. D.; Kapteijn, F.; van Dillen, A. J.; de Jong, K. P. *J. Am. Chem. Soc.* **2006**, *128*, 3956–3964.
- (7) Haruta, M.; Kobayashi, T.; Sano, H.; Yamada, N. *Chem. Lett.* **1987**, 405–408.
- (8) Nkosi, B.; Coville, N. J.; Hutchings, G. J. *J. Chem. Soc., Chem. Commun.* **1988**, 71–72.
- (9) Haider, P.; Kimmmerle, B.; Krumeich, F.; Kleist, W.; Grunwaldt, J. D.; Baiker, A. *Catal. Lett.* **2008**, *125*, 169–176.
- (10) Yang, J.; Tveten, E. Z.; Chen, D.; Holmen, A. *Langmuir* **2010**, *26*, 16558–16567.
- (11) Park, J. Y.; Lee, Y. J.; Khanna, P. K.; Jun, K. W.; Bae, J. W.; Kim, Y. H. *J. Mol. Catal. A: Chem.* **2010**, *323*, 84–90.
- (12) Kim, J. H.; Suh, D. J.; Park, T. J.; Kim, K. L. *Appl. Catal., A* **2000**, *197*, 191–200.
- (13) Pan, H. B.; Wai, C. M. *J. Phys. Chem. C* **2010**, *114*, 11364–11369.
- (14) Itoh, H.; Utamapanya, S.; Stark, J. V.; Klabunde, K. J.; Schlup, J. R. *Chem. Mater.* **1993**, *5*, 71–77.
- (15) Tsoncheva, T.; Ivanova, L.; Rosenholm, J.; Linden, M. *Appl. Catal., B* **2009**, *89*, 365–374.
- (16) Comotti, M.; Li, W. C.; Spliethoff, B.; Schuth, F. *J. Am. Chem. Soc.* **2006**, *128*, 917–924.
- (17) Shen, W. J.; Okumura, M.; Matsumura, Y.; Haruta, M. *Appl. Catal., A* **2001**, *213*, 225–232.
- (18) Rojluetchai, S.; Chavadej, S.; Schwank, J. W.; Meeyoo, V. *Catal. Commun.* **2007**, *8*, 57–64.
- (19) Wyrwalski, F.; Giraudon, J. M.; Lamonier, J. F. *Catal. Lett.* **2010**, *137*, 141–149.
- (20) Pigamo, A.; Besson, M.; Blanc, B.; Gallezot, P.; Blackburn, A.; Kozynchenko, O.; Tennison, S.; Crezee, E.; Kapteijn, F. *Carbon* **2002**, *40*, 1267–1278.
- (21) Zhang, J.; Liu, X.; Blume, R.; Zhang, A. H.; Schlogl, R.; Su, D. S. *Science* **2008**, *322*, 73–77.
- (22) Macia-Agullo, J. A.; Cazorla-Amoros, D.; Linares-Solano, A.; Wild, U.; Su, D. S.; Schlogl, R. *Catal. Today* **2005**, *102*, 248–253.
- (23) Zhu, J. J.; Carabineiro, S. A. C.; Shan, D.; Faria, J. L.; Zhu, Y. J.; Figueiredo, J. L. *J. Catal.* **2010**, *274*, 207–214.
- (24) Wu, Z. S.; Ren, W. C.; Wen, L.; Gao, L. B.; Zhao, J. P.; Chen, Z. P.; Zhou, G. M.; Li, F.; Cheng, H. M. *ACS Nano* **2010**, *4*, 3187–3194.
- (25) Davies, T. E.; Garcia, T.; Solsona, B.; Taylor, S. H. *Chem. Commun.* **2006**, 3417–3419.
- (26) El Kabouss, K.; Kacimi, M.; Ziyad, M.; Ammar, S.; Ensueque, A.; Piquemal, J. Y.; Bozon-Verduraz, F. *J. Mater. Chem.* **2006**, *16*, 2453–2463.
- (27) Brik, Y.; Kacimi, M.; Ziyad, M.; Bozon-Verduraz, F. *J. Catal.* **2001**, *202*, 118–128.
- (28) Busca, G.; Finocchio, E.; Lorenzelli, V.; Ramis, G.; Baldi, M. *Catal. Today* **1999**, *49*, 453–465.
- (29) Ilyas, M.; Saeed, M. *Int. J. Chem. React. Eng.* **2010**, *8*, A79.
- (30) Xie, X. W.; Li, Y.; Liu, Z. Q.; Haruta, M.; Shen, W. J. *Nature* **2009**, *458*, 746–749.
- (31) Rodrigues, C. P.; da Silva, V. T.; Schmal, M. *Appl. Catal., B* **2010**, *96*, 1–9.
- (32) Xie, X. W.; Shen, W. J. *Nanoscale* **2009**, *1*, 50–60.
- (33) Lojewski, J.; Kolodziej, A.; Lojewski, T.; Kapica, R.; Tyczkowski, J. *Appl. Catal., A* **2009**, *366*, 206–211.
- (34) Chan-Thaw, C. E.; Villa, A.; Katekomol, P.; Su, D. S.; Thomas, A.; Prati, L. *Nano Lett.* **2010**, *10*, 537–541.

- (35) Palkovits, R.; Antonietti, M.; Kuhn, P.; Thomas, A.; Schuth, F. *Angew. Chem., Int. Ed.* **2009**, *48*, 6909–6912.
- (36) Palkovits, R.; von Malotki, C.; Baumgarten, M.; Mullen, K.; Baltes, C.; Antonietti, M.; Kuhn, P.; Weber, J.; Thomas, A.; Schuth, F. *ChemSusChem* **2010**, *3*, 277–282.
- (37) Chan-Thaw, C. E.; Villa, A.; Prati, L.; Thomas, A. *Chem.—Eur. J.* **2011**, *17*, 1052–1057.
- (38) Zhu, J. J.; Figueiredo, J. L.; Faria, J. L. *Catal. Commun.* **2008**, *9*, 2395–2397.
- (39) Liotta, L. F.; Di Carlo, G.; Pantaleo, G.; Venezia, A. M.; Deganello, G. *Appl. Catal., B* **2006**, *66*, 217–227.
- (40) Petitto, S. C.; Marsh, E. M.; Carson, G. A.; Langell, M. A. *J. Mol. Catal. A: Chem.* **2008**, *281*, 49–58.
- (41) Jansson, J.; Palmqvist, A. E. C.; Fridell, E.; Skoglundh, M.; Osterlund, L.; Thormahlen, P.; Langer, V. *J. Catal.* **2002**, *211*, 387–397.
- (42) Liu, J.; Zhao, Z.; Wang, J. Q.; Xu, C. M.; Duan, A. J.; Jiang, G. Y.; Yang, Q. *Appl. Catal., B* **2008**, *84*, 185–195.
- (43) Figueiredo, J. L.; Pereira, M. F. R.; Freitas, M. M. A.; Orfao, J. J. M. *Carbon* **1999**, *37*, 1379–1389.
- (44) Xu, Y. J.; Weinberg, G.; Liu, X.; Timpe, O.; Schlogl, R.; Su, D. S. *Adv. Funct. Mater.* **2008**, *18*, 3613–3619.
- (45) Mang, D.; Boehm, H. P.; Stanczyk, K.; Marsh, H. *Carbon* **1992**, *30*, 391–398.
- (46) Paraknowitsch, J. P.; Thomas, A.; Antonietti, M. *J. Mater. Chem.* **2010**, *20*, 6746–6758.
- (47) Paraknowitsch, J. P.; Zhang, J.; Su, D. S.; Thomas, A.; Antonietti, M. *Adv. Mater.* **2010**, *22*, 87–92.
- (48) Mallat, T.; Baiker, A. *Chem. Rev.* **2004**, *104*, 3037–3058.
- (49) Kuhn, P.; Forget, A.; Su, D. S.; Thomas, A.; Antonietti, M. *J. Am. Chem. Soc.* **2008**, *130*, 13333–13337.
- (50) Kuhn, P.; Antonietti, M.; Thomas, A. *Angew. Chem., Int. Ed.* **2008**, *47*, 3450–3453.
- (51) Sheldon, R. A.; Wallau, M.; Arends, I. W. C. E.; Schuchardt, U. *Acc. Chem. Res.* **1998**, *31*, 485–493.
- (52) Son, Y. C.; Makwana, V. D.; Howell, A. R.; Suib, S. L. *Angew. Chem., Int. Ed.* **2001**, *40*, 4280–4283.
- (53) Salavati-Niasari, M.; Bazarganipour, M. *Transition Met. Chem.* **2009**, *34*, 605–612.
- (54) Stuchinskaya, T. L.; Musawir, M.; Kozhevnikova, E. F.; Kozhevnikov, I. V. *J. Catal.* **2005**, *231*, 41–47.